# Tomographic PIV analysis of water tornado flow for environmental system application

**Kazuo Ohmi[1]*, Sudat Tuladhar[2]**

[1] Osaka Sangyo University, Department of Information Systems Engineering, Daito-Osaka, Japan

[2] University of Mississippi, Department of Electrical Engineering, Oxford, MS 38677, USA

*ohmi@ise.osaka-sandai.ac.jp

## Abstract

The 3D pattern and structure of the artificial water tornado flow in a powered water circulatory system (PCS) for environmental protection is investigated by tomographic PIV experiment. The circulatory system aims to promote circulation of deoxygenated bottom layer water in closed water areas such as lakes, ponds and reservoirs. Full 3D-3C analysis of the flow structures of the tornado flow along the boundary and surrounding as well as cross-sectional analysis of the tornado water rise in two orthogonal directions is presented. Some considerations about the practical design of the circulatory system are made regarding the impeller speed and depth for pump-up efficiency.

## 1 Introduction

The 3D flow to be investigated in the present work is the artificial water tornado flow in a powered water circulatory system (PCS) for environmental protection. From the viewpoint of natural water environment protection, the ecological circulation of deoxygenated bottom water in closed water areas (lakes, ponds and reservoirs) is an important task to be considered. While many conventional solutions consume considerable energy to cope with this problem, one of the recent techniques using a PCS (Environment Measurement Services Inc. (2009)) is a simple and energy efficient solution that uses an artificial tornado flow generated by a rotating submerged impeller. Some earlier works provide the 2D-3C PIV analysis of tornado flow in such systems (Hanari and Sakakibara (2010), Ohmi et al. (2013)) but to understand more detailed dynamics of the flow rise, a full 3D-3C PIV analysis of the flow is required.

Also the optimum design parameters of the system, especially the submerged impeller speed and depth remain to be known for maximizing the flow circulation and minimizing the surrounding mixing. In the present work, therefore, the tomographic PIV analysis aims to understand the vortex flow development in a tornado for pump-up efficiency under varied impeller parameters. A cross sectional analysis of the 3D flow structures of tornado flow along the tornado boundary and surroundings is also presented at varied experimental conditions.

## 2 Experimental Setup

As a laboratory model of a close water area, an octagonal water tank has been employed after the reference study of Hanari and Sakakibara (2010). This tank is made of transparent acrylic glass of 352 mm side length (805 mm distance between two parallel sides and 915 mm distance between diagonal corners) and 1000 mm height which is filled up with water up to 950 mm level. The test impeller for tornado generation is 1/20th scale of the real model and is installed at 30 to 60 mm depth from the water surface in the center of the water tank and is driven by a DC servo motor (Oriental Motor Co. Ltd.: BLHM450K) situated above water. The impeller and the servo motor are connected by a vertical axis but separated by a 3 mm thick transparent plate, which covers the entire surface of the water surface and works as a surface

wave canceller. Figure 1 is a schematic diagram of the layout of this water tank with a submerged double decker impeller. The upper and lower impeller elements are both 50 mm in outer diameter, 6 mm in axial thickness and have four vanes in circumferential direction. The planar vanes of the lower element are incident at 45˚, while those of the upper element are at 90˚. In addition, the four vanes of the upper and lower impeller elements are placed with a staggered angle of 45˚.

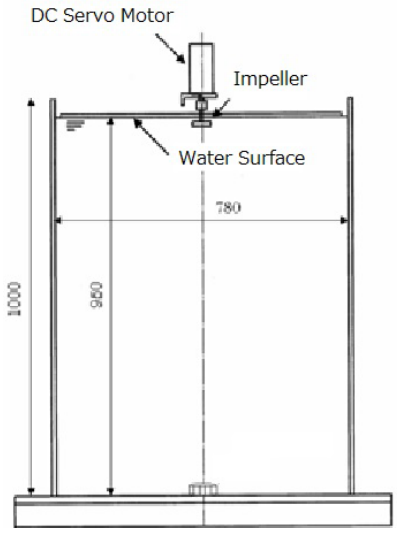


(a) Water tank side view

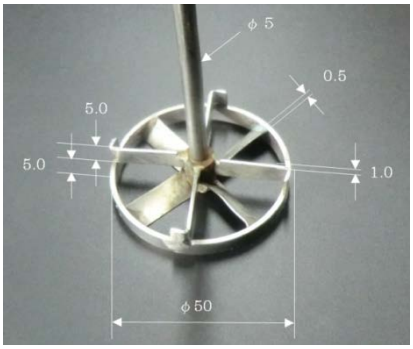


(b) Rotary impeller

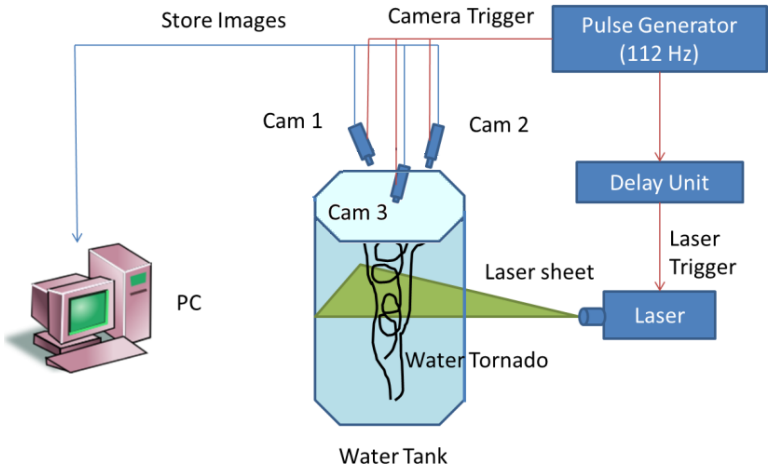


(c) Overview system arrangement

Figure 1: Schematic of experimental setup

For the seeding of PIV experiment, fine porous particles (Mitsubishi Chemical: Sepabeads SP2MGS) of about 120 µm mean diameter were used to observe the tornado flow with swirling of surrounding water inside the tank generated by the submerged impeller. A laser light sheet of about 20 mm thickness at the middle height horizontal cross section of the experimental water tank was used to illuminate the seed particles in the observation volume. A pulse generator operated at 112 Hz was used to send master synchronizing trigger pulse which was then used to trigger the three high-speed cameras externally. The master trigger pulse was divided down to 14 Hz with some delay in order to drive the pulse laser unit. The projection images of the illuminated volume were taken by the three cameras simultaneously and stored in a PC. The water tornado in the PCS was visually located and recorded and then, its behavior was in-

vestigated by tomographic PIV analysis. The effects of two experimental parameters were analyzed by varying the submerged impeller depth (normalized by water tank height) d/H = 0.03 to 0.06 and the rotation speed N = 1000 to 2200 rpm. Each of the high speed cameras (IDT: X-Stream XS-3) were arranged obliquely (approximately 25˚) with respect to the water surface and captured time series grayscale images with 1280×1024 pix resolution and stored them once in on-board memory, then saved them back to storing PC. The angular interval of the axis of the three cameras viewed from above was 120˚. A double pulse Nd:YAG laser with cylindrical lens optics was configured to illuminate a 20 mm thickness volume of the water tank cross section filled with seed particles.

For the tomographic reconstruction using the camera projection images, the measurement volume of 168×168×16 $mm^3$ in physical space was divided into 560× 560×80 voxels, the size of a single voxel being 0.3×0.3×0.2 $mm^3$. The reconstruction algorithm in use was the standard MART (Kak and Staley (1988)) with minor refinement (Joshi et al. 2013) for reducing the computational loads and improving the quality of weighting matrix estimation. After the tomographic reconstruction in 3D voxel space was completed, the displacement of particles at each interrogation point was calculated by means of 3D cross correlation analysis. The 3D cross correlation scheme in use is the parallel projection correlation (PCC) by Bilsky et al. (2011). The interrogation volume size was 32×32×16 voxels with an interval of 8 voxels.

## 3 Experimental Results

3.1 Flow visualization experiment

It had been found in the earlier flow visualization experiment on this type of artificial water tornado (Ohmi et al. 2013) that the water tornado after initial generation undergoes a highly characteristic evolution of vortex flow as shown in Figure 2. This cycle of vortex development and breakdown was iterated autonomously with a period of about 4 to 10 minutes depending on the impeller speed. Therefore the present tomographic PIV experiment was focused on such a flow evolution to understand the mechanism of vortex development and breakdown in tornado and thereby to improve the pump-up circulation efficiency of the PCS. The latter objective was basically achieved by the pursuit of optimized values for the two system parameters of PCS (submerged impeller speed and depth) for efficient tornado flow rise and minimum dissipation mixing in the surroundings.

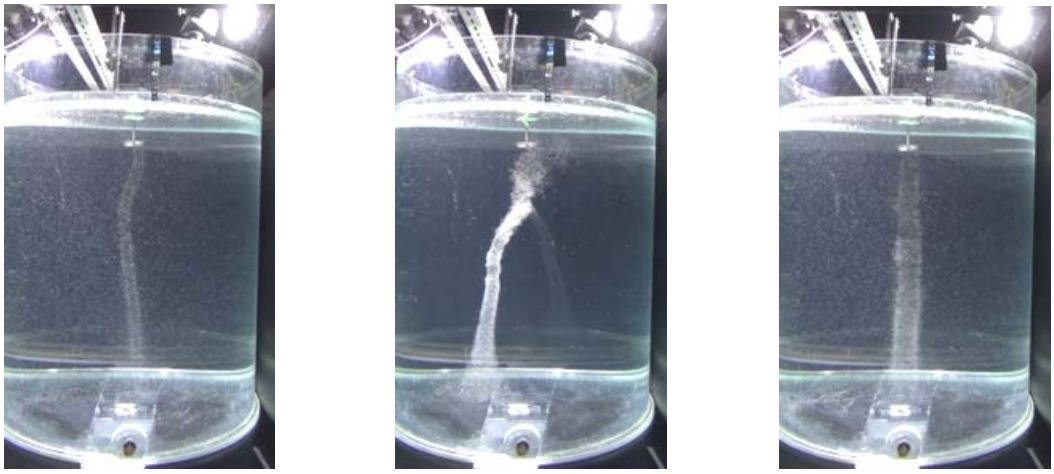

(a) Full development (b) Breakdown (c) Reorganization

Figure 2: Time evolution of water tornado flow

3.2 Tomographic reconstruction

The tomographic reconstruction of 3D tornado flow is performed on the basis of raw recorded images without any post-processing. The extent of reconstruction volume is rather restricted with respect to the

camera recorded image because of the temporally unstable locations of tornado center in the view field of each viewing camera. Figure 3 (a), (b) and (d) show 3D angle, top and side views of the tomographic reconstruction result, indicating the position of (binary) particles, of the water tornado at full development stage. By contrast, Figure 3 (c) shows 3D angle view of the tomographic reconstruction result at post breakdown stage. In general, the tornado flow at full development stage is characterized by highly concentrated seed particles along the outer edge of the rotating water tornado. This is most probably due to the centrifugal force induced by the enforced rotating flow as well as due to the strong velocity gradient along the circumferential part of the water tornado. By contrast, the tornado flow at post breakdown stage is characterized by rather dispersed seed particles along the edge of the rotating water tornado. Not only that, the seed particles at this stage are found less actively distributed around the water tornado probably because of the attenuated centrifugal force and thereby the velocity gradient along the circumferential part of the tornado. The location of the tornado center in the reconstruction volume is slowly moving in time steps as is the tornado center in the camera recorded image.

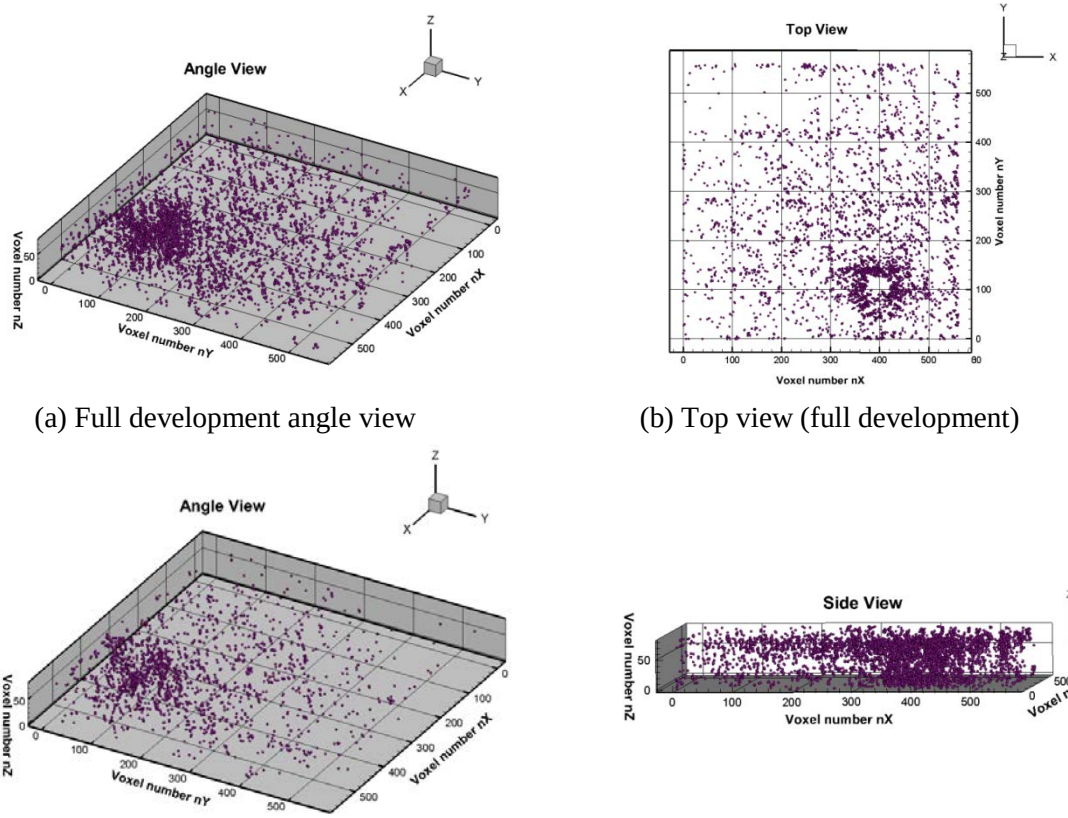


(a) Full development angle view (b) Top view (full development)

(c) Post breakdown angle view (d) Side view (full development)

Figure 3: Tomographic reconstruction results of 3D particles in the observation volume

3.3 Velocity and vorticity distribution at full development stage

Figure 4 shows the tomographic PIV results of the tornado flow at full development stage. The impeller speed $N$ is 1800 rpm and the normalized impeller depth is 0.06. The first diagram is a volume view of 3D velocity plots and $z$-vorticity contours of the tornado flow at full development, while the second one is a vertical cross sectional view of the same parameters at four orthogonal planes. In both cases, the measurement volume is 168×168×16 $mm^3$ in physical scale, which is divided into a discretized space of 560×560×80 voxels, of which the single voxel size is 0.3×0.3×0.2 $mm^3$ in $x$, $y$ and $z$ directions.

In Figure 4 (b), the four vertical cross-sections are located across the tornado outer boundary which clearly depicts the counter clock-wise swirl of the tornado-flow at a given height of the tornado. This cross

sectional view also shows that similar nature of tornado flow rise is observed at every cross sectional height of the tornado. Most of the green (near zero vorticity) surrounding part does not have any swirling motion and contribute little towards any undesirable mixing of the sediments to the neighborhood. Very small tornado rising and falling can be seen outside the tornado boundary that contributes very little towards the mixing in the surroundings.

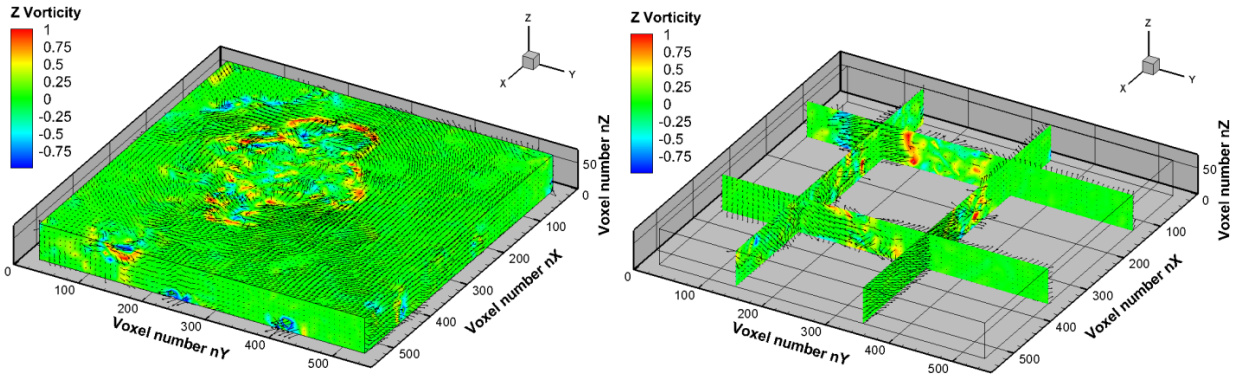


(a) Volume view (b) Cross sectional view at four orthogonal planes

Figure 4: 3D velocity plots and *z*-vorticity contours of the tornado flow at full development stage

3.4 Tornado flow characteristics at different heights

The relevant tomographic PIV experiment shows the characteristics of tornado flow at bottom, mid and top horizontal cross sections at full development stage. The distribution of positive and negative vorticity along the tornado outer boundary is more or less similar at three positions, inferring the fact that the uprising of flow inside the tornado is consistent at various height levels, which further depicts the stability of swirling motion across various cross sections. The cross sectional velocity profiles at the outer boundary of tornado are not axisymmetric but rather oval with a small degree of circumferential undulation. And the extent of this outer boundary and the circumferential undulation are gradually increased as the tornado goes upwards. However, at each of the three cross sections, the flow rise in the nearby regions outside the tornado boundary is almost neutral, whereas that in more outer regions is rather fluctuating. This may provide a good performance of the PCS for circulation of bottom water with minimum dissipation mixing of sediments.

3.5 Effects of impeller speed

The relevant tomographic PIV experiment shows the tornado flow at different impeller speed $N$ from 1000 to 2200 rpm with an increment of 200 rpm at a fixed impeller depth of $d/H$ = 0.06. The formation of established tornado flow starts at impeller speed of 1000 rpm, where a small swirling motion with minimum concentration of vorticity is present. With the rise in the impeller speed from 1000 to 1800 rpm, the swirling motion and the vorticity concentration around the tornado periphery are increased, giving rise to higher tornado flow rise with minimum disturbance in the surroundings. Above the impeller speed of 1800 rpm, the tornado flow rise is increased by a very small extent but the surrounding disturbance becomes much higher. The time evolution of tornado flow at impeller speed of 1000 rpm is also found to be the most stable.

3.7 Effects of impeller depth

The relevant tomographic PIV experiment shows the tornado flow at different impeller depth $d/H$ from 0.03 to 0.06 with an increment of 0.01 at the optimum impeller speed of 1800 rpm. Normalized impeller depth less than 0.03 is practically not feasible due to insufficient clearance between the impeller and the water surface plate, causing heavy cavitation that prevents efficient operation of the impeller. Also, normalized depth larger than 0.06 is avoided due to the technical limitation of impeller design. The

formation of small tornado flow rise is started from $d/H = 0.03$, which is however not sufficient to produce sufficient flow rise for proper water extraction. In the course of this experiment with varied impeller depth, it is observed that the tornado flow rise at maximum normalized depth of $d/H = 0.06$ produces most stable and established dynamic characteristics.

## 4 Conclusion

In the present study, a full 3D-3C analysis of a water tornado flow rise induced by submerged rotating impeller in a powered water circulatory system (PCS) was carried out using a tomographic PIV technique. The flow characteristics of the tornado flow during the full development and post breakdown stages were shown in the positional reconstructions as well as in the velocity and vorticity maps. Formation of highly increased circumferential velocity areas with strong velocity gradient along the outer edge of the tornado swirling flow was shown in the velocity reconstructions. The cross sectional velocity distribution of the water tornado was found to be not axisymmetric but rather oval with a small degree of circumferential undulation. Regarding the two experimental parameters relative to the PCS design, namely the submerged impeller speed and normalized depth, the 3D PIV results at different heights showed that the maximum tornado flow rise with minimum dissipation mixing toward the surroundings was attained at 1800 rpm impeller speed with 0.06 normalized depth. Thus, the tomographic PIV technique was found to be very helpful and effective technique to investigate the characteristics of the structure of tornado flow rise in the powered water circulatory system.

## Acknowledgements

The present authors are grateful to Osaka Sangyo University for the financial support of Bunyabetsu grant-in-aid for the fiscal year 2015.

## References

Abdel-Aziz YI and Arara HM (1971) Direct linear transformation from comparator coordinates into object space coordinates in close-range photogrammetry. *Proc. of the ASP Symposium on Close-Range Photogrammetry*: 1-18.

Bilsky A, Dulin V, Lozhkin V, Markovich D, and Tokarev M (2011) Two-dimensional correlation algorithms for tomographic PIV, *Proc. 9th International Symposium on Particle Image Velocimetry*: 2-222.

Elsinga GE, Scarano F, Wieneke B, and Van Oudheusden BW (2005) Tomographic particle image velocimetry. *Proc. 6th International Symposium on Particle Image Velocimetry*: S10-1.

Environment Measurement Services Inc. (2009) EcoFlow document. http://www.ems-kankyo.co.jp/ecoflow/en-punhu.pdf

Hanari T, and Sakakibara J (2010) Dual-plane stereo-PIV study on tornado-like vortex in water (in Japanese). *Journal of Visualization Society Japan*, 30(7): 47-54.

Herman GT, and Lent A (1976) Iterative reconstruction algorithm. *Computers in Biology and Medicine*, 6(4): 273-294.

Joshi B, Ohmi K, and Nose K (2012) Novel algorithms of 3D particle tracking velocimetry using a tomographic reconstruction technique, *Journal of Fluid Science and Technology*, 7: 242-258.

Kak AC, and Staley M (1988) Principles of computerized tomographic imaging. IEEE Press.

Ohmi K, Hiratsuka A, and Sasaki M (2013) Visualization experiment on an artificial tornado flow under density stratified water environment. *Proc. 12th Asian Symposium on Visualization*: 229.